

# Design of DC Voltage Control for D-STATCOM

Kittaya Somsai, Thanatchai Kulworawanichpong, and Nitus Voraphonpiput

**Abstract**— This paper presents the DC voltage control design of D-STATCOM when the D-STATCOM is used for load voltage regulation. Although, the DC voltage can be controlled by active current of the D-STATCOM, reactive current still affects the DC voltage. To eliminate this effect, the control strategy with elimination effect of the reactive current is proposed and the results of the control with and without the elimination the effect of the reactive current are compared. For obtaining the proportional and integral gains of the PI controllers, the symmetrical optimum and genetic algorithms methods are applied. The stability margin of these methods are obtained and discussed in detail. In addition, the performance of the DC voltage control based on symmetrical optimum and genetic algorithms methods are compared. Effectiveness of the controllers designed was verified through computer simulation performed by using Power System Tool Block (PSB) in SIMULINK/MATLAB. The simulation results demonstrated that the DC voltage control proposed is effective in regulating DC voltage when the D-STATCOM is used for load voltage regulation.

**Keywords**—D-STATCOM, DC voltage control, Symmetrical optimum, Genetic algorithms

## I. INTRODUCTION

IN a power distribution system, controlled reactive power sources are commonly used for load voltage regulation. Due to their high control bandwidth, D-STATCOMs, based on three-phase pulse width modulation voltage source converters, have been proposed for this application [1] – [3]. For a fast control, the D-STATCOM is usually modeled using the  $dq$  axis theory for balanced three-phase systems, which allows definition of instantaneous reactive current and instantaneous magnitude of phase voltages [4]. In addition, the current controller design is developed using a rotating  $dq$  frame of reference that offers higher accuracy than the stationary frame techniques [5].

Most literature on the D-STATCOM and STATCOM control concentrates in control of the output current and DC voltage regulation for a given reactive current reference. The current decoupling control based on  $dq$  reference frame received considerable attention in [6] – [8]. The authors presented a remarkable advance by letting the  $d$ -axis always be coincident with the supply voltage; first prototypal control where active and reactive powers are decoupled was realized. In addition, an alternative approach using a linearized state space model in the D-STATCOM and STATCOM control design was proposed in [9] – [10].

In this paper, a modeling strategy similar base on the rotating  $dq$  reference frame is used. The D-STATCOM DC voltage control strategy with elimination term of reactive current is proposed. The symmetrical optimum design is applied to obtain the proportional gain and integral time of PI controllers. The response of the D-STATCOM current with and without the decoupling are compared. Performance of the

propose model and the controller design were verified using computer simulation performed in SIMULINK/MATLAB.

## II. D-STATCOM CONFIGURATION AND MODELING

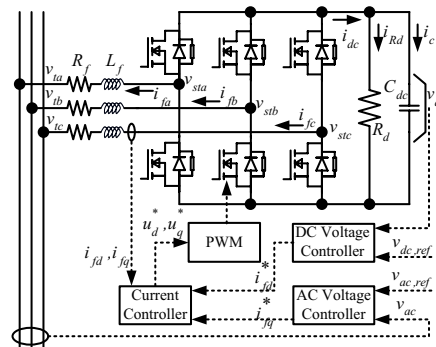


Fig. 1 Basic circuit diagram and control of the D-STATCOM system

The basic circuit diagram and control of the D-STATCOM system are shown in Fig. 1. It consists of a three phase voltage source converter (VSC), interfacing inductors, dc link capacitor, and control systems. The VSC is connected to the network through the transformer and the interfacing inductors which are used to filter high-frequency components of compensating currents. The inductance  $L_f$  in this figure represents the leakage inductance of the transformer and the interfacing inductors. The copper loss of the connecting transformer and loss of the interfacing inductor are represented by a resistance  $R_f$ . As seen in Fig. 1, the D-STATCOM output AC voltage is represented by  $v_{st,abc}$ . This voltage is generated by the converter and is assumed to be quasi-sinusoidal voltage waveform. Therefore, voltage equation of AC system can be written as

$$L_f \frac{di_{f,abc}}{dt} = -R_f i_{f,abc} - v_{t,abc} + v_{st,abc} \quad (1)$$

Consider the DC system in Fig. 1, the DC current  $i_{dc}$  consists of capacitor current  $i_c$  and resistor current  $i_{Rd}$ . The resistor  $R_d$  represents losses in the converter. The power flow into the converters equals to the instantaneous power of the DC capacitor which can be described as

$$P_{dc} = v_{dc} i_{dc} = v_{dc} (i_c + i_{Rd}) = P_{ac} = v_{st,abc}^T i_{f,abc} \quad (2)$$

Here,  $v_{dc}$  is the D-STATCOM DC voltage,  $i_f$  is the D-STATCOM output current,  $v_l$  is the load voltage, while the subscript “*abc*” implies vectors consisting of individual phase quantities. From Fig. 1, the relation between DC power and AC power can be expressed as

$$v_{dc} \left( C_{dc} \frac{dv_{dc}}{dt} + \frac{v_{dc}}{R_{dc}} \right) = - \left( v_{st,abc}^T i_{f,abc} \right) \quad (3)$$

where  $C_{dc}$  is the DC link capacitance. After applying the three-phase to two-phase transformation and followed by the rotational transformation with the chosen  $dq$  reference frame that described in [11], the D-STATCOM dynamics in (1) and (3) can be rewritten as:

$$\frac{di_{fd}}{dt} = -\frac{1}{T_f} i_{fd} + \omega i_{fq} - \frac{1}{L_f} v_{ld} + \frac{1}{L_f} k_p u_d v_{dc} \quad (4)$$

$$\frac{di_{fq}}{dt} = -\frac{1}{T_f} i_{fq} - \omega i_{fd} + \frac{1}{L_f} k_p u_q v_{dc} \quad (5)$$

$$\frac{dv_{dc}}{dt} = -\frac{v_{dc}}{T_{dc}} - \frac{3}{2} \frac{1}{C_{dc}} k_p u_d i_{fd} - \frac{3}{2} \frac{1}{C_{dc}} k_p u_q i_{fq} \quad (6)$$

where  $T_f$  is the time constant of the transformer and interfacing inductor,  $T_f = L_f / R_f$  while  $T_{dc}$  is the time constant of the DC system,  $T_{dc} = C_{dc} R_{dc}$ . Here,  $k_p u_d v_{dc}$  and  $k_p u_q v_{dc}$  represent the D-STATCOM output AC voltage on  $d$ -axis and  $q$ -axis ( $v_{st,d}$  and  $v_{st,q}$ ), respectively. Meanwhile, the  $\omega$  is the synchronous angular speed of the system,  $v_{dc}$ ,  $i_{fd}$  and  $i_{fq}$  represent the state variables of the D-STATCOM,  $k_p$  is a constant value depending on the type of converter and transformer ratio [16]. The D-STATCOM output AC voltage can be generated by control the converter. Therefore, AC voltage command on  $dq$ -axis ( $u_d$  and  $u_q$ ) are the control inputs of the D-STATCOM.

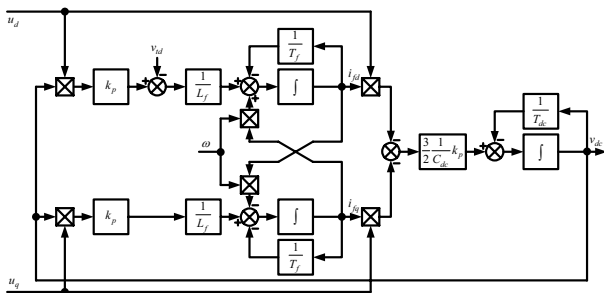


Fig. 2 Basic circuit diagram and control of the D-STATCOM system

Block diagram of the D-STATCOM can be modified from equation (4) to (6) as shown in Fig. 2. This block diagram

represents the model of the AC system and the converter of the D-STATCOM on the synchronously rotating reference frame ( $dq$ -axis). This system has two inputs that are the AC voltage command on  $dq$ -axis. The active current, reactive current and DC capacitor voltage are the state variables of this system.

### III. CONTROL ALGORITHM

#### A. Current Control Strategy

The equations in (4) and (5) are used for designing the D-STATCOM current controller. These equations clearly show that the D-STATCOM output currents are induced by its output voltage modulation. However, the current control of the converter on the synchronously rotating reference frame ( $dq$ -axis) is a two-input two-output system with cross coupling between the active and reactive current. To eliminate this coupling, decouple control for the active and reactive current proposed in [8] is applied. The current control structure for the D-STATCOM in this paper is shown in Fig. 3. Since the current control with decoupling is applied, the D-STATCOM currents with cross coupling between the active and reactive currents can be separately represented on  $d$ -axis and  $q$ -axis. Therefore, the transfer function of the current control loop each axis can be simplified as:

$$G_{cl,i}(s) = \frac{1}{sT_{ei} + 1} \quad (7)$$

Where  $T_{ei}$  is an equivalent time constant of the current control loop.

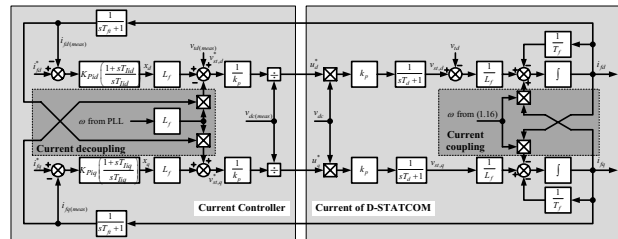


Fig. 3 Current Control structure for the D-STATCOM

#### B. DC Voltage Control Strategy

In this paper, the control objective is to keep the DC voltage around its reference when the D-STATCOM is used for load voltage regulation. This objective cannot be achieved directly by  $u_d$  through (6) as there might be possibility of  $i_{fd}$  going to zero during a transient. However, the DC voltage can be regulated indirectly by controlling  $i_{fd}$ . Although, the DC voltage can be controlled by  $i_{fd}$ ,  $i_{fq}$  still affects the DC voltage as there exists the term of  $u_q i_{fq}$  in (6). To eliminate this effect, (6) can be modified as:

$$\frac{dv_{dc}}{dt} + v_{dc} = -x_{dc} \quad (8)$$

where the term  $u_q i_{fq}$  is included in  $x_{dc}$  as

$$x_{dc} = \frac{3}{2} \frac{1}{C_{dc}} k_p (u_d i_{fd} + u_q i_{fq}) \quad (9)$$

Equation (9) shows that the DC voltage is increased following the transient with negative  $x_{dc}$ . Based on this principle, the control action  $x_{dc}$  can be expressed as:

$$x_{dc} = -K_{pvdc} \left( \frac{1+sT_{Ivdc}}{sT_{Ivdc}} \right) (v_{dc}^* - v_{dc}) \quad (10)$$

where the proportional-plus-integral (PI) regulators are used to control the DC voltage in the present work. The proportional controller (P) will affect the steady state error and rise time. An integral controller (I) controls the transient response and the steady state error. Since the control action  $x_{dc}$  is determined by (10), the D-STATCOM active current command  $i_{fd}^*$  in (9) can be rearranged as:

$$i_{fd}^* = - \left( \frac{2C_{dc} x_{dc}}{3k_p} + u_q i_{fq} \right) \left( \frac{1}{u_d} \right) \quad (11)$$

The DC voltage control structure and the D-STATCOM's DC voltage are demonstrated in Fig. 4. The active current command  $i_{fd}^*$ , accounting for the DC voltage regulation, can be generated by the DC voltage controller with the DC voltage deviation as the input. This  $i_{fd}^*$  is used as the input of the current control loop,  $G_{cl,i}(s)$ , then the controlled active current results in the DC voltage which enables the DC voltage control.

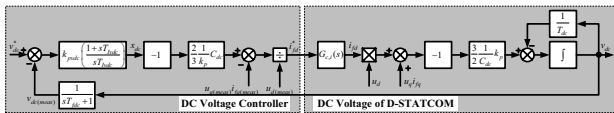


Fig. 4 DC voltage control structure and the D-STATCOM DC voltage.

As seen from Fig. 4, the control loop is a cascade control in which the DC voltage control is a main control loop and the current control is an auxiliary control loop. The main control loop is superimposed on the auxiliary control loop. This means that the current control is substantially faster than the DC voltage control. To simplify this design, it is assumed that the time delay of the feedback filter and the equivalent time constant of the current control loop ( $T_{ei}$ ) are combined as

$$T_e = T_{fdc} + T_{ei} \quad (12)$$

Hence, the simplify open loop transfer function of the DC voltage  $v_{dc}$  with respect to the output of PI controller of DC control  $x_{dc}$  is given as

$$G_{vdcopen}(s) = \left( \frac{T_{dc}}{sT_{dc} + 1} \right) \left( \frac{1}{sT_e + 1} \right) \quad (13)$$

C. DC Voltage PI Controller Design based on symmetrical optimum methods

The PI controllers' parameters depend on the parameters of the open loop transfer function (i.e., natural frequency ( $\omega_0$ ), damping coefficient ( $\zeta$ ), and pole value (p)). In general,  $\omega_0$  and  $\zeta$  characterize the desired system behavior and they are arbitrarily constant, while the location of poles can be chosen. The specific pole locations can be imposed by using supplementary conditions. The conditions for choosing the pole locations refer to the symmetrical optimum method, which simplifies the expressions of the PI parameters. The goal of this scheme is to find the pole locations of the closed-loop transfer function, which satisfy the assumptions given by the symmetrical optimum design around  $\omega_0$ , for the transfer function of open-loop system.

The symmetric optimum method is suitable for an open-loop transfer function of a third-order polynomial in the denominator. Consider the classical control loop, as shown in Fig. 5. The controller is of PI type as described in (14). If the plant includes a delay whose time constant is more than four times as large as the sum of the time constants of the remaining delays ( $T_1 > 4T_e$ ) as described in (15), then the large delay acts, as a first approximation, like an integrator.

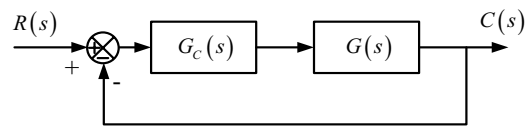


Fig. 5 Classical control system

$$G_c(s) = K_p \left( \frac{1+sT_I}{sT_I} \right) \quad (14)$$

$$G(s) = \frac{k_1}{(sT_1+1)(sT_e+1)} \quad (15)$$

The proportional gain and integral time constant of the PI controller can be calculated in the following forms [12], [13]:

$$K_p = \frac{T_1}{2k_1T_e} \quad (16)$$

$$T_I = 4T_e \quad (17)$$

D. DC Voltage PI Controller Design based on Genetic Algorithms (GAs) methods

There exist many different approaches to tune PI

controller's parameters. The GAs is well-known [14-16] and there exist a hundred of works employing the GAs technique to design the controller in various forms. The GAs is a stochastic search technique that leads a set of population in solution space evolved using the principles of genetic evolution and natural selection, called genetic operators e.g. crossover, mutation, etc. With successive updating new generation, a set of updated solutions gradually converges to the real solution. Because the GAs is very popular and widely used in most research areas [15-17] where an intelligent search technique is applied, it can be summarized briefly as shown in the flowchart of Fig. 6 [16].

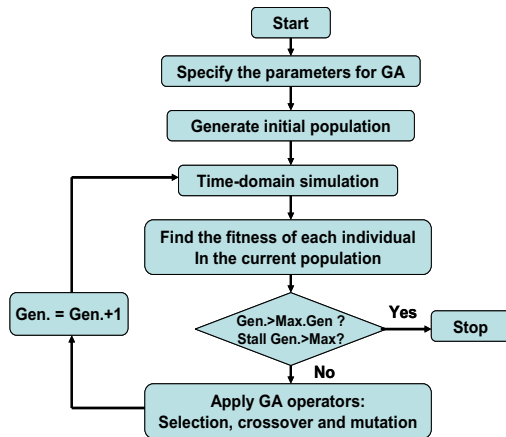


Fig. 6 Flowchart of GAs procedures

In this section, the GAs is selected to build up an algorithm to tune  $K_{Pvdc}$  and  $K_{Ivdc}$  parameters of the DC voltage control. The procedure to perform the proposed parameter tuning is described as follows. First, time-domain results of magnitude and frequency swing obtained by simulating the DC voltage control system in SIMULINK are obtained. Second, the Genetic Algorithms (GADS TOOLBOX) is employed to generate a set of initial random parameters. With the searching process, the parameters are adjusted to give response of best fitting close to the desired response. To perform the searching properly, its objective function is the key. In case of tuning PI controller's parameters of the DC voltage control based on GAs, the objective function is defined in (18).

$$\int_0^{t_{sim}} |\Delta v_{dc}(t)| dt \quad (18)$$

where  $\Delta v_{dc} = y_{desired}(v_{dc}) - y_{simulated}(v_{dc})$

$y_{desired}(v_{dc})$  is the desired response of the DC voltage.

$y_{simulated}(v_{dc})$  is the simulated response of the DC voltage.

By using MATLAB/SIMULINK, the DC voltage control block diagram of this section can be formed graphically as presented in Fig. 4. Meanwhile, the current control is an auxiliary control loop that the block diagram is shown in Fig. 3. In this section, two cases of the DC voltage controller i.e. the DC voltage controller with non-elimination and elimination term of  $u_q i_{fq}$  are used. For  $K_{Pvdc}$  and  $K_{Ivdc}$  parameters of the DC voltage control tuning based on the GAs, the D-STATCOM is used for load voltage regulation when the source voltage ( $V_s$ ) sag, i.e.  $V_s$  from 12.1 kV to 8.47 kV and 8.47 kV to 12.1 kV.

For design the DC voltage control of the D-STATCOM, the parameters in Table I are used. Given that sum of the small time constant  $T_v = 0.0004$ , the PI controller's parameters of the DC voltage control based on the symmetrical optimum method can be obtained by using (16) and (17) as shown in Table II. Meanwhile, with 30 computational trials in each test case of the parameter tuning based on the GAs, one trial is selected to present the convergence characteristic of the PI tuning algorithm as shown in Fig. 7. In addition, the PI controller's parameters of the DC voltage control based on the symmetrical optimum method and the best parameters obtained by GAs for each test case are put in Table II.

TABLE I  
PARAMETERS

| D-STATCOM parameters                                      |                           |
|---|---------------------------|
| Interfacing resistance and inductance ( $R_f$ and $L_f$ ) | 0.01 $\Omega$ and 5.07 mH |
| Constant value of converter ( $k_p$ )                     | 1.00                      |
| DC link capacitance ( $C_{dc}$ )                          | 150 $\mu$ F               |
| Capacitor leakage resistance ( $R_{dc}$ )                 | 61.273 k $\Omega$         |
| Switching frequency ( $f_{sw}$ )                          | 10 kHz                    |
| Current Control parameters                                |                           |
| $K_{Pid} = K_{Piq}$                                       | 5,000                     |
| $T_{Iid} = T_{Iiq}$                                       | 0.0004                    |
| $T_{fi} = T_d$  | 0.0001                    |

TABLE II  
PI PARAMETERS OF DC VOLTAGE CONTROL FOR EACH TEST CASE

| DC voltage controller                   | $K_{Pvdc}$       | $T_{Iiq}$         | Cost      |
|---|------------------|-------------------|-----------|
| Symmetrical optimum methods             |                  |                   |           |
| 1. non-elimination term of $u_q i_{fq}$ | 1,250<br>(Fixed) | 0.0016<br>(Fixed) | 17,360.36 |
| 2. elimination term of $u_q i_{fq}$     | 1,250<br>(Fixed) | 0.0016<br>(Fixed) | 14,248.11 |
| Genetic Algorithms (GAs) methods        |                  |                   |           |
| 1. non-elimination term of $u_q i_{fq}$ | 3,840.56         | 0.000502          | 8,334.94  |
| 2. elimination term of $u_q i_{fq}$     | 3,370.82         | 0.000500          | 7,819.37  |

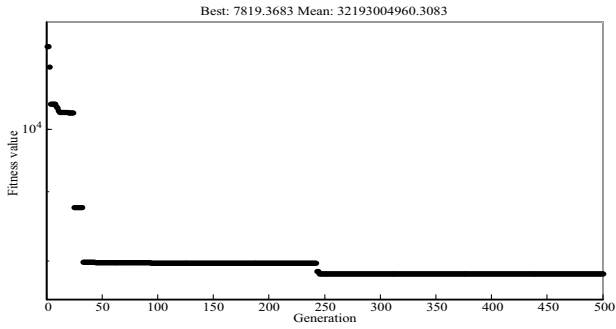


Fig. 7 Convergence of the PI parameter tuning using MATLAB's GADS TOOLBOX for the first 500 consecutive generations

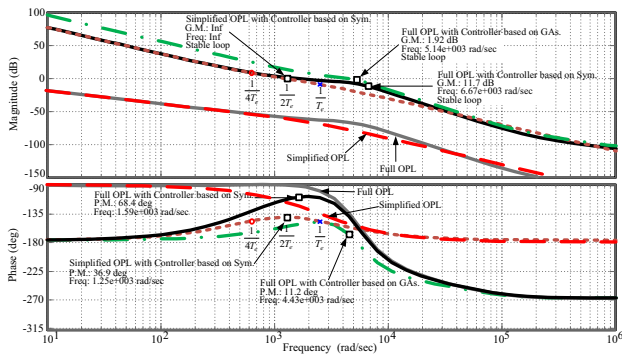


Fig. 8 Bode plot of open loop transfer function with PI controller

In addition, the Bode plots of the DC voltage control based on symmetrical optimum and genetic algorithms methods are compared as shown in Fig. 8. It is to clarify the concept of symmetrical optimum. Fig. 8 shows the frequency characteristics (Bode plot) of the individual system elements in the DC voltage control loop. The Dot line trace for the modulus of the open-loop transfer function in (13) with DC voltage control based on symmetrical optimum method which shows symmetry of the corner points  $1/4T_e$  and  $1/T_e$  with respect to the gain crossover frequency  $1/2T_e$  on the 0 dB line. If the control loop is adjusted in accordance with the symmetrical optimum, the behavior is dependent on the sum of the time constants of the small delays in the control loop. However, the Bode plot of full open-loop transfer function (obtained by including the DC voltage control in Fig. 4 and the current control loop in Fig. 3) with DC voltage control based on symmetrical optimum method is indicated by solid line as shown in Fig. 8. Meanwhile, the dot-dash line presents the Bode plot of full open-loop transfer function with the DC voltage control based on genetic algorithms method.

Furthermore, from this figure, gain and phase stability margin of the full open-loop transfer function with DC voltage control based on symmetrical optimum and genetic algorithms methods can be obtained and compared. It is seen that gain and phase crossover frequency of the DC voltage control based on symmetrical optimum method are 1,590 and 6,670 rad/sec, respectively while that of the DC voltage control based on genetic algorithms method are 4,430 and 5,140

rad/sec, respectively. The gain and phase stability margin of the DC voltage control based on symmetrical optimum method are 11.7dB and 68.4 deg, respectively whereas that of the DC voltage control based on genetic algorithms method are 1.92 dB and 11.2 deg, respectively. These results demonstrate the DC voltage control based on symmetrical optimum method gives a better stability margin.

#### IV. SIMULATION RESULTS AND DISCUSSION

Effectiveness of the controllers designed above was verified through computer simulation performed by using Power System Tool Block (PSB) in SIMULINK/MATLAB. The DC voltage controllers with and without the elimination term of  $u_q i_{fq}$  are compared. The performance of the proposed DC voltage control is studied in case of the D-STATCOM used for load voltage regulation when the source voltage is varied. The schematic diagram of a D-STATCOM for load voltage regulation is shown in Fig. 9 and parameters of the system are shown as Table III. From the simulation results, the following observations are made.

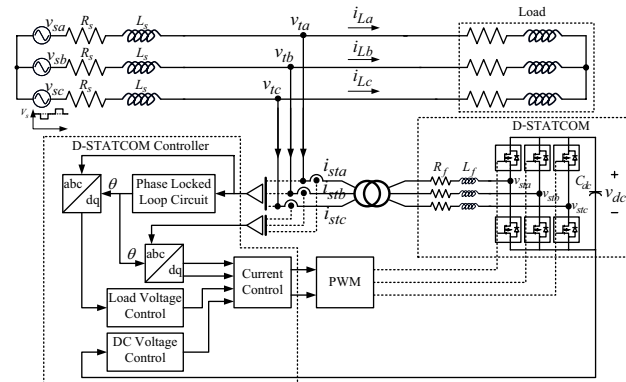


Fig. 9 Distribution system with the installed D-STATCOM

TABLE III  
PARAMETERS OF THE POWER DISTRIBUTION SYSTEM

| The distribution power system parameters             |                      |
|--|----------------------|
| Nominal source voltage ( $V_s$ )                     | 12.1 kV              |
| Desired load voltage magnitude ( $V_{ld}^*$ )        | 11.00 kV             |
| Source resistance and inductance ( $R_s$ and $L_s$ ) | 1 $\Omega$ and 10 mH |
| Load resistance ( $R_l$ )                            | 10 $\Omega$          |
| System frequency ( $f_s$ )                           | 50 Hz                |

##### A. Performance of DC Voltage Control based on Symmetrical Optimum Method

The performance of DC voltage control based on symmetrical optimum method when the D-STATCOM is used for load voltage regulation is shown in Fig. 10. At  $t = 0.05$  sec, source voltage is changed from 12.10 kV to 8.47 kV and at  $t = 0.1$  sec it is changed from 8.47 kV to 12.10 kV. Meanwhile, at  $t = 0.25$  sec it is changed from 12.10 kV to 16.33 kV and at  $t = 0.35$  sec it is changed from 16.33 kV to 12.10 kV. The load voltage, compensator currents and DC voltage are shown in Fig. 10(a) to Fig. 10(c), respectively. In addition, Fig. 10(c)

compares the performance of the DC voltage control with and without the elimination term of  $u_q i_{fq}$ . As can be seen in this figure, the DC voltage control with the elimination term of  $u_q i_{fq}$  gives the best dynamic response. This control also gives smaller settling time and also smaller overshoot. However, it is not significant.

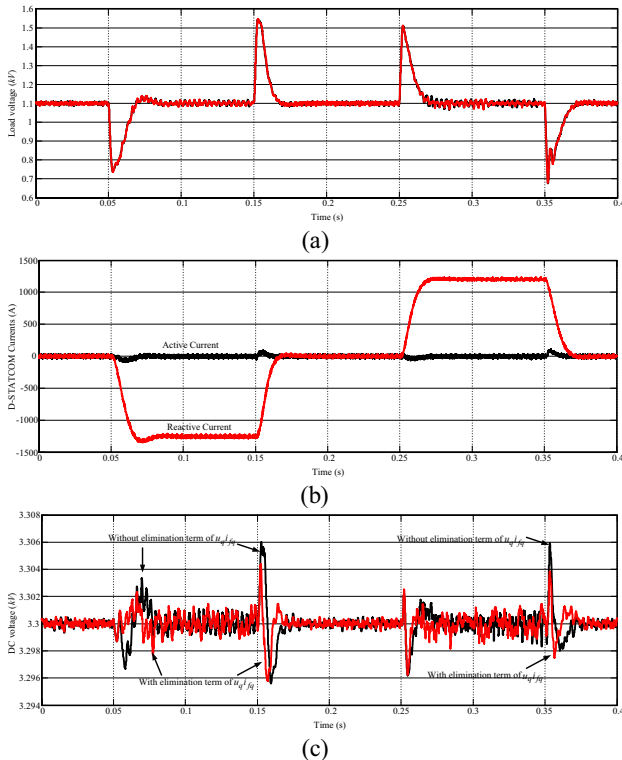


Fig. 10 Performance of DC control based on symmetrical optimum method

### B. Performance of DC Voltage Control based on genetic algorithms Method

Similar to case A, the D-STATCOM is used for load voltage regulation when the source voltage is varied. Fig. 11 shows the DC voltage when the DC voltage control based on genetic algorithms method. In this figure, responses of the DC voltage control with and without the elimination term of  $u_q i_{fq}$  are compared. As seen in this figure, the response of the DC voltage of both DC voltage control are not difference.

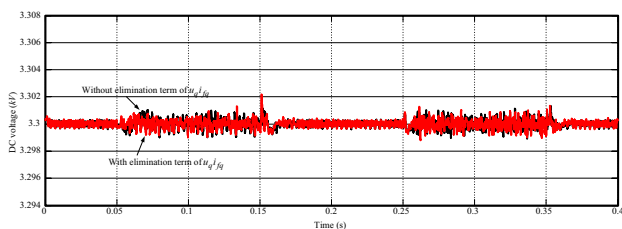


Fig. 11 DC voltage when DC control based on genetic algorithms method

### C. Comparison of Performance of DC Voltage Control based on Symmetrical Optimum and genetic algorithm Methods

In this case, the performance of the DC voltage control based on symmetrical optimum and genetic algorithms methods are compared as shown in Fig. 12. It is seen in this figure that the DC voltage control based genetic algorithms gives the best dynamic response. The DC voltage control based genetic algorithms also gives smaller overshoot. However, The DC voltage control based symmetrical optimum also gives better stability margin.

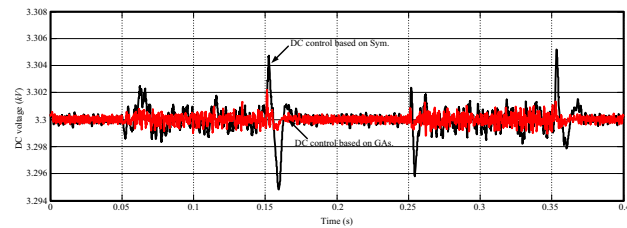


Fig. 12 Comparison the DC voltage of DC control based on Symmetrical optimum and genetic algorithms method

## V. CONCLUSION

This paper proposed the DC voltage control design of D-STATCOM when the D-STATCOM is used for load voltage regulation. The symmetrical optimum and genetic algorithms methods are applied to obtain the proportional and integral gains of the PI controllers. The DC voltage control with and without elimination term of  $u_q i_{fq}$  are investigated and compared. In comparison, the simulation results showed that the DC voltage control based on the symmetrical optimum method with elimination term of  $u_q i_{fq}$  gives a better performance in transient states. However, the responses of the DC voltage control based on the genetic algorithms method with and without elimination term of  $u_q i_{fq}$  are not difference.

In addition, the performance of the DC voltage control based on symmetrical optimum and genetic algorithms methods are compared. It is seen that the DC voltage control based genetic algorithms gives the best dynamic response. The DC voltage control based genetic algorithms also gives smaller overshoot. However, The DC voltage control based on symmetrical optimum also gives better stability margin.

## ACKNOWLEDGMENT

One of the authors, Mr. Kittaya Somsai, would like to thank the office of the Higher Education Commission, Thailand for supporting a grant fund under the program Strategic Scholarships for Frontier Research Network for the Joint Ph.D Program Thai Doctoral degree for this research.

## REFERENCES

- [1] A. Ghosh, and G. Ledwich, *Power quality enhancement using custom power devices*. Massachusetts: Kluwer Academic, 2002.
- [2] P. S. Sensarma, K. R. Padiya, and V. Ramanarayanan, "Analysis and Performance Evaluation of a Distribution STATCOM for Compensating Voltage Fluctuations," *IEEE Trans. Power Del.*, vol. 16, no. 2, pp. 259 – 264, 2001.

- [3] C. Hochgraf, and R. H. Lasseter, "Statcom controls for operation with unbalanced voltages," *IEEE Trans. Power Del.*, vol. 13, no. 2, pp. 538 – 544, 1998.
- [4] C. Schauder, and H. Mehta, "Vector analysis and control of advanced static VAr compensators," *Proc. Inst. Elect. Eng. C, Gen. Transm. Distrib.*, Jul 1993, pp. 299 – 306
- [5] E. Acha, V. G. Agelidis, O. Anaya-Lara, and T. J. E. Miller, *Power Electronic control in Electrical system*, Oxford: Reed Educational and Professional, 2002.
- [6] C. Schauder, M. Gernhardt, E. Stacey, T. Lemak, L. Gyugyi, T.W. Cease, and A. Edris, "Development of  $\pm 100$  MVar static condenser for voltage control of transmission systems," *IEEE Trans. Power Deliv.*, vol. 10, no. 3, pp. 1486 – 1496, 1995.
- [7] Woei-Luen Chen, Wei-Gang Liang, and Hrong-Sheng Gau, "Design of a mode decoupling STATCOM for voltage control of wind-driven induction generator systems," *IEEE Trans. Power Deliv.*, vol. 25, no. 3, pp. 1758 – 1767, 2010.
- [8] M. G. Molina, and P. E. Mercado, "Control design and simulation of DSTATCOM with energy storage for power quality improvements," *IEEE/PES Transmission & Distribution Conf. Exposition*, Latin America, TDC '06, 15-18 August 2006, pp. 1 – 7.
- [9] C. K. Sao, P. W. Lehn, M. R. Iravani, and J. A. Martinez, "A benchmark system for digital time-domain simulation of a pulse-width-modulated D-STATCOM," *IEEE Trans. Power Deliv.*, vol. 17, no. 4, pp. 1113 – 1120, 2002.
- [10] P. W. Lehn, and M. R. Iravani, "Experimental evaluation of STATCOM closed loop dynamics," *IEEE Trans. Power Deliv.*, vol. 13, no. 4, pp. 1378 – 1384, 1998.
- [11] A. Jain, K. Joshi, A. Behal, and N. Mohan, "Voltage regulation with STATCOMs: modeling, control and results," *IEEE Trans. Power Deliv.*, vol. 21, no. 2, pp. 726 – 735, 2006.
- [12] Friedrich Frohr and Fritz Orthenburger, *Introduction to electronic control engineering*. New Delhi: Second Wiley Eastern Reprint, 1992.
- [13] Marian P. Kazmierkowski, R. Krishnan, and Frede Blaabjerg, *Control in power electronics selected problems*. California: Elsevier Science, 2002.
- [14] M. Rashidi, F. Rashidi, and H. Monavar, "Tuning of power system stabilizers via genetic algorithm for stabilization of power system," *IEEE Int. Conf. Systems, Man and Cybernetics*, Vol. 5, 5-8 October 2003, pp. 4649-4654.
- [15] T. Kulworawanichpong, K-L.Areerak, K-N. Areerak, P. Pao-la-or, P. Puangdownreong, and S. Sujitjorn, "Dynamic parameter identification of induction motors using intelligent search techniques," *The 24<sup>th</sup> IASTED Int. Conf. Modelling, Identification, and Control (MIC 2005)*, Austria 2005, pp. 328-332.
- [16] T. Charuwat, and T. Kulworawanichpong, "Genetic based distribution service restoration with minimum average energy not supplied," *The 8<sup>th</sup> International Conference on Adaptive and Natural Computing Algorithms (ICANNGA2007)*, 11-14 April 2007, pp. 230-239.
- [17] Y.P. Wang, D.R. Hur, H.H. Chung, N.R. Watson, J. Arrilaga, and S.S. Matair, "A genetic algorithms approach to design an optimal PI controller for static VAr compensator," *Int. Conf. Power System Technology (PowerCon 2000)*, Vol. 3, 4-7 December 2000, pp. 1557-1562.